PNAS
www.pnas.org

Supplementary Information for

Constraining the atmospheric limb of the plastic cycle

Janice Brahney[1*+], Natalie Mahowald[2*+], Marje Prank[2,3], Gavin Cornwell[4], Zbigniew Klimont[5], Hitoshi Matsui[6], Kimberly Ann Prather[7]

Janice Brahney, janice.brahney@usu.edu

Natalie M. Mahowald, mahowald@cornell.edu

This PDF file includes:

Supplemental text: Additional sensitivity studies.

As stated in the text, we add an additional sensitivity study where the a priori information about the size of the road and braking source is included based on (29). Unfortunately, this is the first study to consider other atmospheric sources, and thus there is no information to include. To include a priori information about the strength of this source, and its error, we use a Bayesian approach and add a term to the cost function:

$$\chi^2 = \sum_j \left[\frac{(y_{model,j} - y_{obs,j})}{\sigma_j}\right]^2 + P + \frac{(S_r - S_m)^2}{\sigma_s} \quad \text{(eq. 1)}$$

Where S_r is the ***a priori*** best estimate with the uncertainty (σ_s) from (29) or 284 (102-787) Gg yr^{-1}, and S_m is our estimate. The uncertainties bars on their estimate are not symmetric, but since their value is larger than ours, we use the lower limit estimate (284-102=182 Gg yr-1) for our σ_s. The rest of the variables are identical to the approach in the main text, but repeated here: yobs,j are the 316 observations, and ymodel,j is found using the following equation:

$$y_{model,j} = \sum_i S_i * R_{i,j}$$

Where Ri,j is the modeled relationship between each source (i) and the deposition at each site (j). P represents a penalty which is assessed if any of the sources become negative. The magnitude of this is set to force all the estimations to result in positive values. The σj is the model-observational error or uncertainty in each observation, when compared against the model. This will be the sum of direct observational error, in addition to the error in the model's ability to represent accurately the observation.

Including the very uncertain a priori information does not significantly shift our 95% uncertainty estimates, although it does result in a quantitively different answer (Figure S6).

Our second supplemental sensitivity study is to use a slightly different ocean distribution for our inversion. In the base case we deduce from flow convergence the location of the buildup of plastics, and matched these to estimates from van Sebille et al. (10) for basin averages, while in the ocean sensitivity study we directly use the van Sebille et al. (10) estimate of ocean plastics based on <5mm sizes as our spatial distribution. The two distributions are qualitatively similar, but in details they are different (especially the Arctic), but both provide similar optical estimations for the final strength of the ocean sources, which is very uncertain (Figure S6).

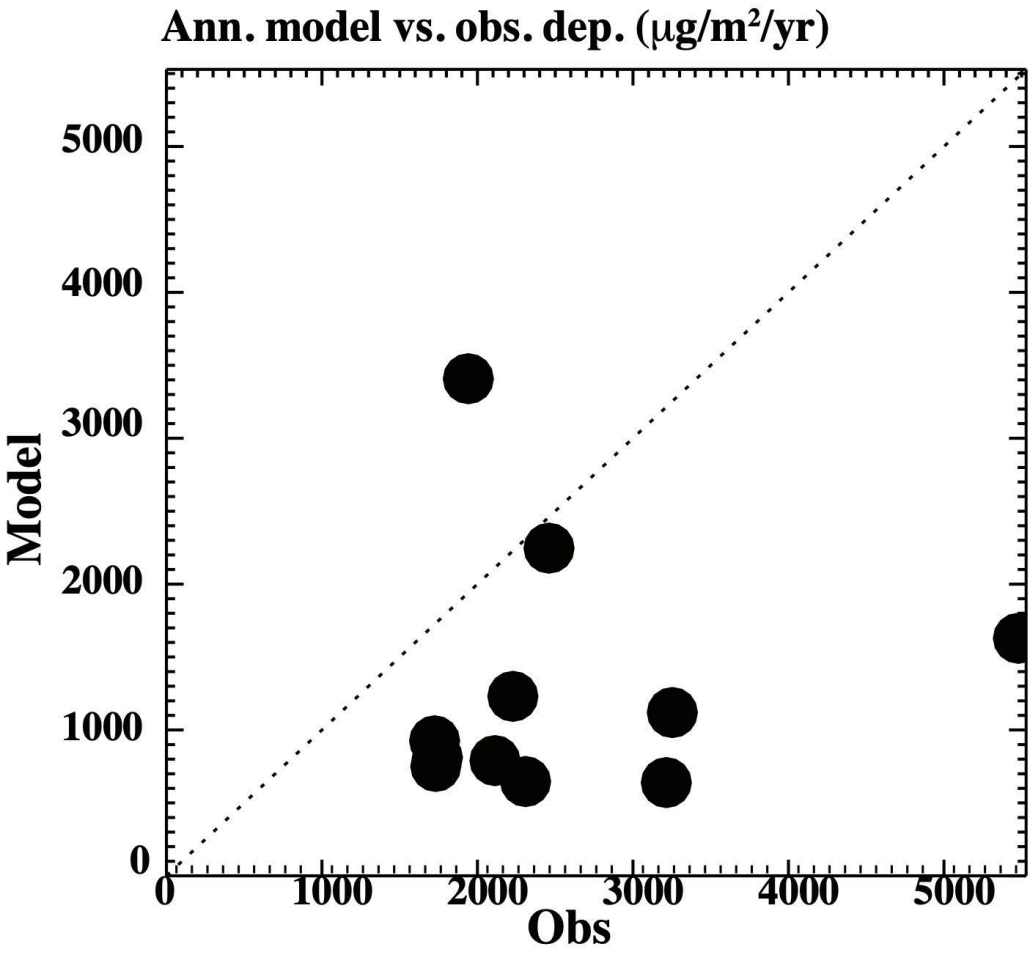

Fig. S1. Scatter plot of annual average plastic deposition data at each station compared to the best fit of the model at the 11 different sites (shown in Figure 3a) (r=-0.33, n=11).

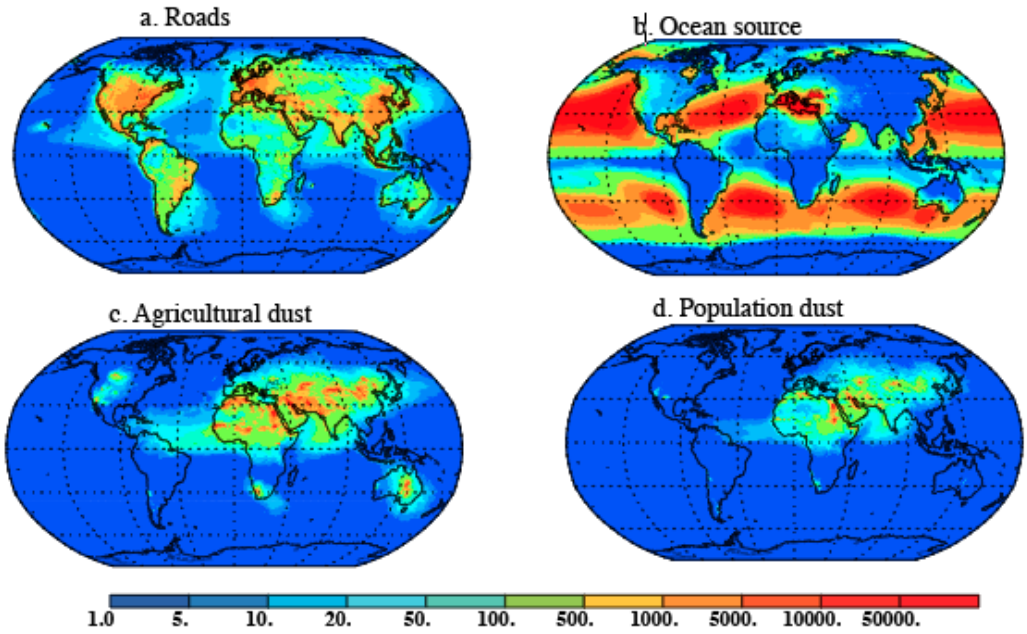

Fig. S2. The contribution of plastic deposition from each source to the model (µg/m2/year) globally for the (a) Road source, (b) Ocean source, (c) Agricultural Dust, and (d) Population Dust source. Since the population source is estimated to be zero for the base case, this is not plotted.

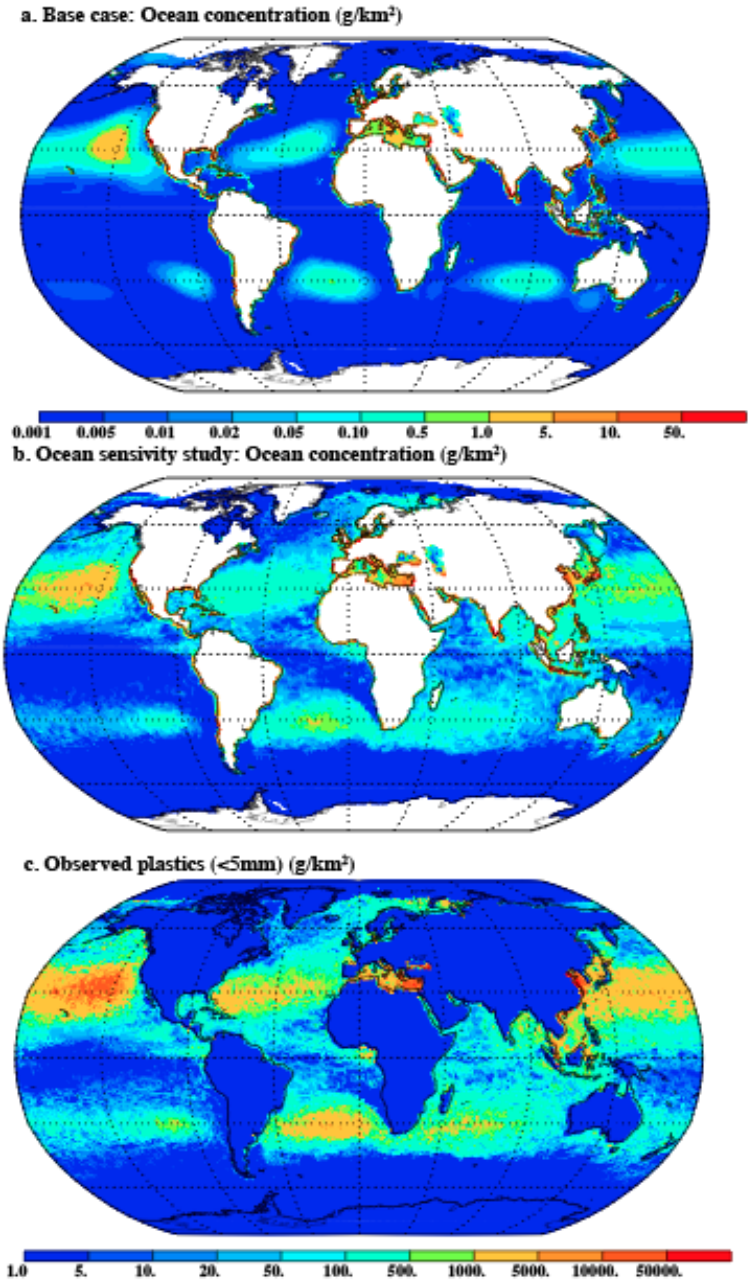

Fig. S3. Deduced ocean surface concentrations of microplastic using base case (a) Notice that the spatial distribution of this source is fixed based on gyre strength and van Sebille et al. 2016, as described in the Methods. (b) Estimated ocean surface concentration using the ocean sensitivity study (which uses the spatial distribution directly from van Sebille et al., 2016), and (c) the estimate of microplastic concentration, which are all plastics collected in trawling (~<5mm). Notice that the top two panels (a and b) use the same color bar, but c) uses a very different color bar (100x larger scale).

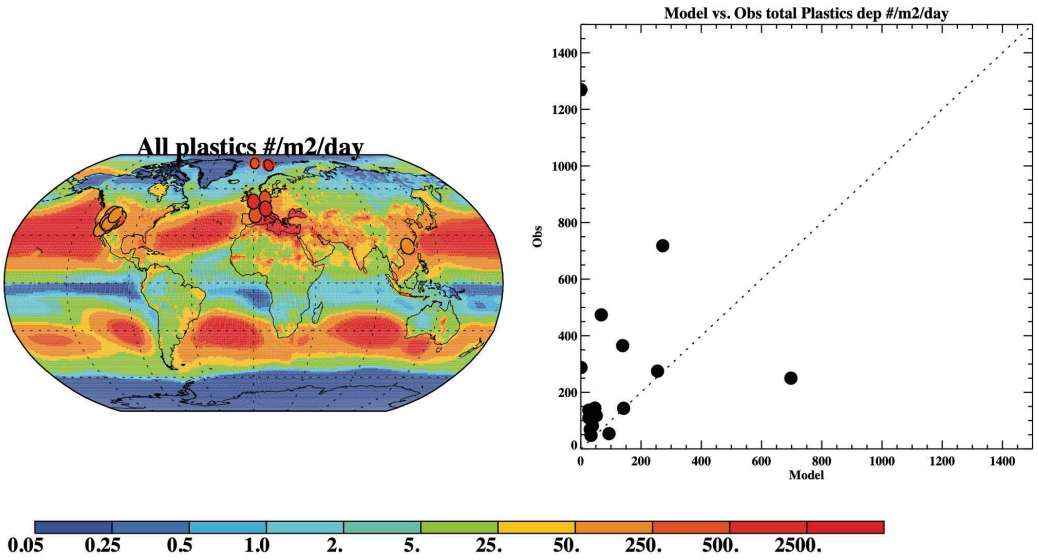

Fig. S4. Comparison of modeled microplastic deposition against available observations (#/m^2/day). Observational data comes from (1–6).

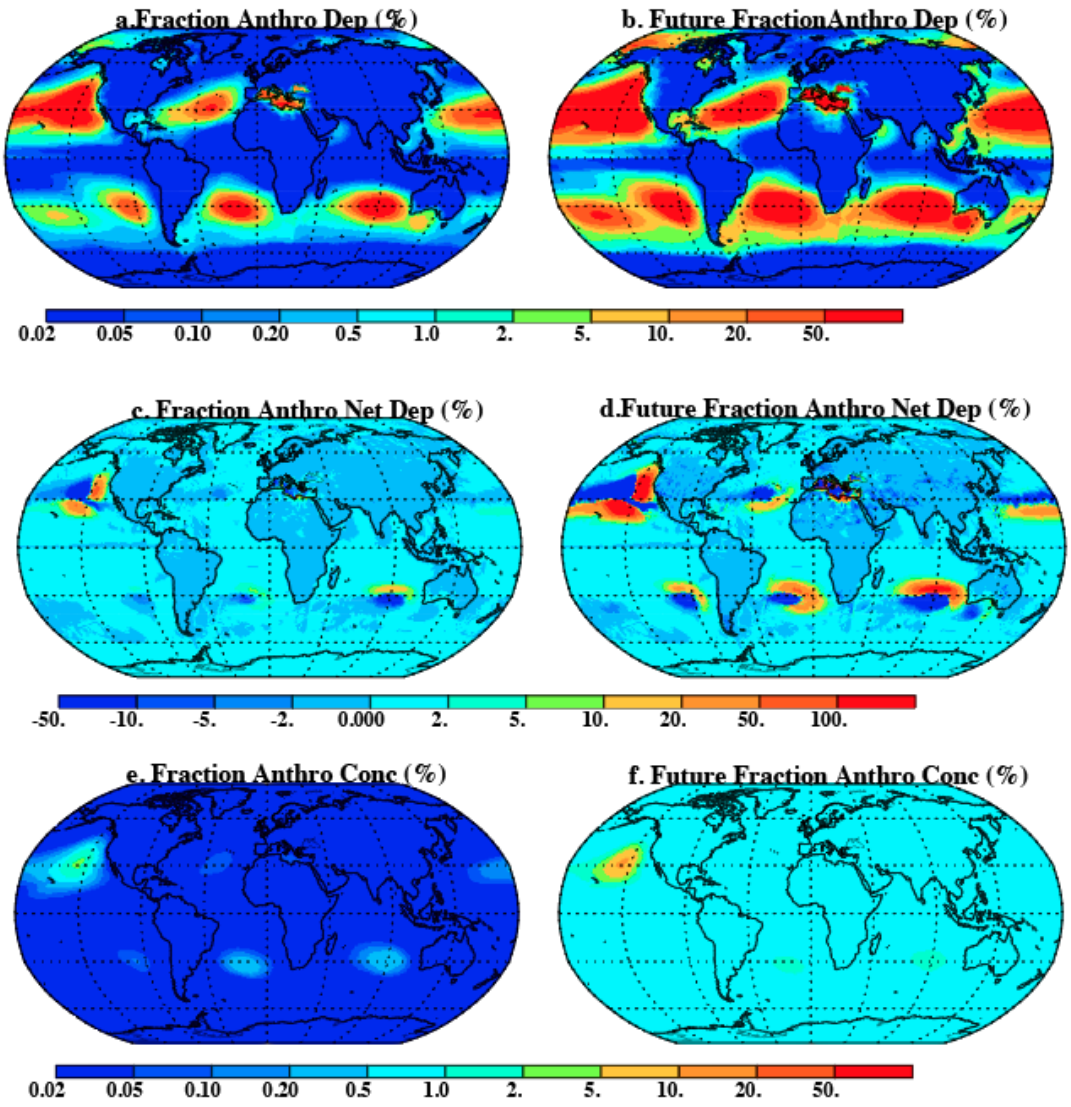

Fig. S5. Estimated current (a) and future (b) (assume 10x higher) fraction of gross deposition that is polymeric (%) as current deposition of plastics/total anthropogenic particle deposition. Total anthropogenic particles include black carbon, organic carbon, sulfate, and agricultural dust (to be conservative, we assume that all black carbon, organic carbon and sulfate are anthropogenic, although there were some deposition of these in preindustrial era (7)). Since much of the plastic deposition over the open ocean comes from upwind in the ocean, we also plot the % of the net deposition (deposition-source)/total anthropogenic deposition for (c) current and (d) future (assume 10x higher). Model estimated % current (e) and future (f) fraction of surface concentrations of anthropogenic aerosols that is polymeric (%).

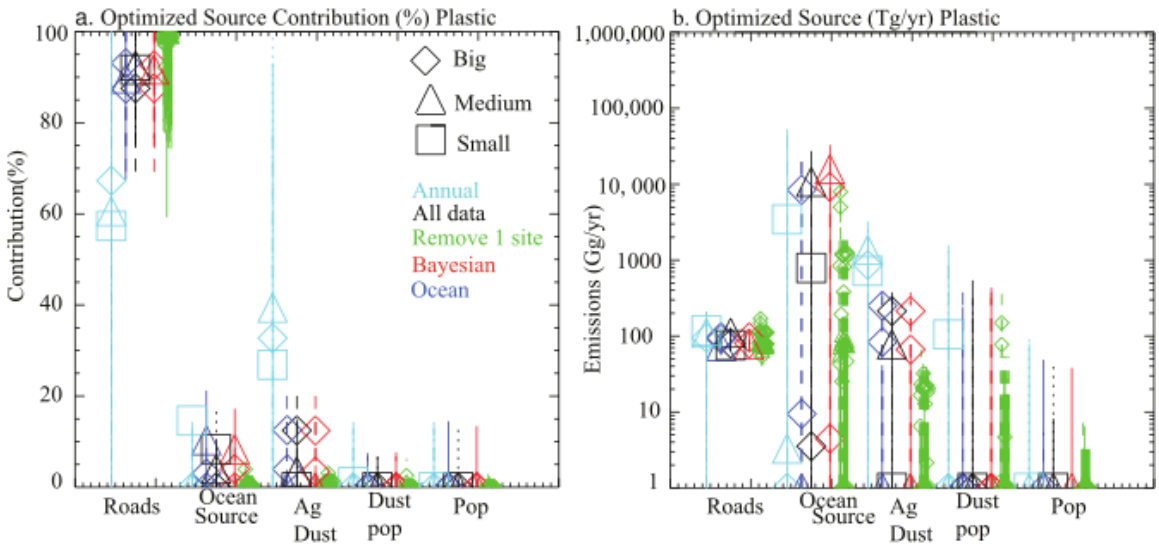

Figure S6: Comparison of the optimal estimation method with the sensitivity studies.

Similar to Figure 2b for (a), and figure 4a for (b).: (a) Estimates of the contribution at the observing sites from different sources as inferred using the method described in the Methods section for the three sizes: big (diamond), medium (triangle), and small (square). For all sources and cases, the 95% confidence limits are shown as vertical lines. Multiple sensitivity studies were conducted (see Methods for details), with time averaging (cyan), and with each site withheld (green), showing the ranges of values that can be obtained for each relative source strength. New sensitivity study including a priori information about the sources (red), or with a different ocean source distribution (blue). (b) Globally average source of microplastics (a), as inferred using the method described in the Methods section for the three sizes: big (diamond), medium (triangle), and small (square). For all sources, the 95% confidence limits are shown as vertical lines. Multiple sensitivity studies were conducted (see Methods for details), with time averaging (cyan), and with each site withheld (green), showing the ranges of values that can be obtained for each source strength extrapolated globally. New sensitivity study including a priori information about the sources (red), or with a different ocean source distribution (blue).

Table S1. Evaluation of optimal model simulations of plastics against available data, including wet and dry deposition (2). Station name, abbreviation from the NADP network, latitude, longitude, observational mean value, model mean value, correlation coefficient at each station, and number of observations.

		Mean ($\mu g/m^2/yr$)	Mean ($\mu g/m^2/yr$)		
		Obs.	Model.	Correlation Coefficient	Number of Obs.
All data		1306	699	0.12	316
Observing stations	Station Abr. (Lat. Lon.)				
Grand Canyon National Park (NP), AZ	AZ03 (36.1°N 247.8°E)	1001	578	0.09	26
Joshua Tree NP, CA	CA67 (34.1°N 243.6°E)	1105	1511	-0.30	19
Indian Peaks, CO	CO02 (40.1°N 254.4°E)	1145	1928	0.49	17
East River, CO	CO10 (39.0°N 253.0°E)	1634	630	0.28	42
Rocky Mountain NP, CO	CO98 (40.3°N 254.4°E)	2253	639	0.59	44
Craters of the Mood NP, ID	ID03 (43.5°N 246.5°E)	1393	542	-0.21	25
Great Basin NP, NV	NV05 (39.0°N 245.8°E)	1045	688	0.45	31
Canyonlands NP, UT	UT09 (38.46°N 250.2°E)	858	479	-0.04	27
Unita National Forest (NF), UT	UT95 (40.8°N 250.5°E)	1340	655	-0.22	20
Bryce Canyon NP, UT	UT99 (37.6°N 247.8°E)	1095	457	-0.14	34
Wind River , WY	WY06 (42.9°N 250.2°E)	774	428	0.38	31
Annual average		1240	776	-0.03	11

Table S2. Model evaluation for dust and sea spray aerosols at the observing stations.

	Variable	Mean ($\mu g/m^2/day$) Obs.	Mean ($\mu g/m^2/day$) Model	Correlation Coefficient	Number of obs	% error
Wet deposition	Dust	9.50	9.35	0.15	213	0.79
Wet deposition	Na	0.088	0.053	0.18	213	24.75
Dry deposition	Dust	21.9	5.51	0.07	103	59.83

Table S3. Source strength of optimal estimation for the base case by bin in Tg/year of microplastics. Aerodynamic size of the microplastics are shown (inside parenthesis)

	Roads	Ocean	Ag dust	Pop dust
Bin 1 (0.3μm)	0.00070	0.00033	0.00001	0.000
Bin 2 (2.5μm)	0.0067	0.0035	0.0029	0.001
Bin 3 (7μm)	0.020	0.029	0.011	0.003
Bin 4 (15μm)	0.024	0.098	0.016	0.004
Bin 5 (35μm)	0.023	1.09	0.019	0.005
Bin 6 (70μm	0.022	7.3	0.020	0.006
Total	0.096	8.6	0.069	0.018

Table S4. Lifetime of different modeled sources in days. Aerodynamic size of the microplastics are shown (inside parenthesis)

	Roads	Ocean	Ag dust	Pop dust
Bin 1 (0.3μm)	2.96	1.72	6.83	6.07
Bin 2 (2.5μm)	2.80	1.68	6.60	5.99
Bin 3 (7μm)	1.43	1.04	2.84	2.73
Bin 4 (15μm)	0.45	0.45	0.79	0.75
Bin 5 (35μm)	0.08	0.14	0.14	0.13
Bin 6 (70μm	0.04	0.08	0.07	0.06
Total	0.65	0.10	0.96	0.94